Proceedings of the ASME 2009 International Mechanical Engineering Congress and Exposition
IMECE2009
November 13-19, 2009, Lake Buena Vista, Florida, USA

IMECE2009-10403

ABLATION AND SEPARATION OF DERMIS VIA ULTRA-SHORT PULSED LASER

Huan Huang
Department of Mechanical and Aerospace Engineering, Rutgers University
Piscataway, NJ 08854, USA

Zhixiong Guo
Department of Mechanical and Aerospace Engineering, Rutgers University
Piscataway, NJ 08854, USA
E-mail: guo@jove.rutgers.edu

ABSTRACT

Dermal tissue ablation and layer-separation with minimal thermal damage to the surrounding tissue via an ultra-short pulsed (USP) laser has been investigated. At first, a parametric study for wet tissue surface line ablation was investigated. The line features were measured by both microscope and scanning electron microscopy. The dermis ablation threshold and the incubation factor were determined through the line ablation results. It is found that a general microscope may give inflated ablation line width. Following the ablation experiment, histological view of ablated wet tissue samples with different combinations of laser parameters has been undertaken to obtain proper laser parameters for tissue separation with minimal thermal damage. The separation of a whole piece of wet dermal tissue into two thin layers was presented. A thin dermal tissue layer pushing to 220 μm thickness was obtained.

1. INTRODUCTION

Since the invention in 1960 lasers have been of great interest in applications to medical community [1] and have become irreplaceable tools of modern medicine, spanning a wide spectrum of applications in many current medical procedures, vision correction [2], soft tissue surgery [3,4], and optical imaging [5,6]. Laser ablation that takes great advantages in precise material removal is a promising method in processing and treatment of biological tissues [7,8], biodegradable polymers [9-11], collagen gels [12], dental implants [13], etc. At low laser flux, the material is heated through linear absorption of the laser energy and evaporates or sublimates, the plasma formation is either initiated or supported by thermionic emission of free electrons. In this case, the target is usually shielded by the formed plasma on the target surface and impedes further energy deposition by linear absorption. At high laser flux, the material is typically converted to plasmas by non-linear absorption and causes rapid phase transition. This is different from mechanism of thermal ablation for continuous wave (CW) or long pulsed lasers [14, 15]. One describes the effect as a strong local ionization of the medium, where the plasma reaches density beyond a critical value. Energy is very efficiently absorbed, and the local plasma temperature increases dramatically. An explosive Coulombian expansion producing cavitation follows, and forms a very powerful and damaging shockwave that develops on nanosecond timescale. Besides, the shielding effect for USP laser pulse is not a major factor for laser energy delivery. If the rate of plasma formation is relatively slow, in the ns time regime (for ns excitation laser pulses) or longer, energy is transferred from the plasma to the lattice owning to heat diffusion, so thermal damages like melting or charring of the surrounding tissue is commonly observed.

In the ultra-short time regime (from picoseconds or down to femtoseconds pulse duration), the plasma expansion happens on a timescale smaller than the rate of energy transfer to the lattice, and thermal damages are reduced or eliminated [8]. Plasma-mediated ablation is a completely different process of laser-tissue interaction compared with thermal ablation. The so-called plasma-mediated ablation occurs when the incident energy flux is over the threshold for optical breakdown ($>10^{11}$ W/cm^2 in liquids and solids) and it can be achieved easily in the focal spot of the laser beam for USP lasers since the pulse duration is ultra-short, while it is not easy to be achieved by CW or long pulsed lasers. Furthermore, the substantial plasma generation and absorption enable the ablation of materials that are normally difficult to ablate by continuous wave or ns pulsed lasers, such as transparent or low absorption materials [11].

Thus, efficient processing of almost all tissue types via the USP laser plasma-mediated ablation is possible. These distinct features make USP lasers very attractive for separating or cutting tissues. In a previous study [11], the authors have demonstrated clean and clear separation and fabrication of polydimethylsiloxane (PDMS) thin layers and networks without collateral damage via the USP laser plasma-mediated ablation.

Meanwhile, naturally derived materials such as allograft, xenograft, and autograft tissues have many biological, chemical and mechanical advantages over synthetic materials; and thus, hold tremendous potential for use in tissue transplantation and therapies. The number of patients recovering from post-burn and post-traumatosis by graft tissue implantation is growing and nowadays over 900,000 allografts are transplanted each year in USA. However, surgical treatment is frequently restricted by the scarcity of adequate tissues available for reconstruction. Separation of a tissue into two or multiple layers leads to augmented usages of the limited tissues, doubling or even tripling the harvest of donor tissues. Moreover, a tissue may have to be separated into layers, as the tissue in its entirety may not be necessary or appropriate for implantation [16]. In the treatment of burn wounds, for instance, in many cases it is necessary only to implant the epidermal layer of a skin allograft [17]. It is also known that in many cases only an acellular dermis is needed, e.g., in facial soft tissue augmentation [18] or breast reconstruction [19].

Before transplanted into a patient or subject, these natural biomaterials typically requires chemical or physical pretreatment for sterilization and immunogenicity reduction and other processing, such as preparing the tissue by cutting and shaping the tissue into an appropriate form [16-20]. However, there lack effective and efficient methods for separating natural tissues into thin layers and for precisely cutting and shaping tissues without collateral damage [16], saying by experts in the Musculoskeletal Transplant Foundation (MTF), the largest tissue bank in USA. Techniques using a mechanical tool or surgical knife to separate a tissue into multiple layers or cut the tissue into portions are often limited in precision, resulting in a large amount of waste. It is noticed that those mechanical tools can also cause damage to the underlying layers and surrounding tissues to the range of 0.1 to 1 mm. For chemical method, it is time-consuming and the residues at the tissue sample could be hard to remove and harmful for the safety of further usage. Thus, it would be very useful to develop an effective method that can precisely and non-intrusively modify tissues with minimized damage.

In this article, we report extended investigations on the fundamentals of USP laser ablation of human dermis and application to dermal tissue separation and cutting. Firstly, parametric studies for wet tissue surface line ablation were conducted to characterize the ablation threshold at wet dermis surface. The ablation widths and depths resulting from different laser parameters were compared. Then the effects of laser parameters such as pulse overlap rate and pulse energy on the ablation efficiency of tissue were also investigated. Furthermore, histological views of the ablated wet dermis samples were presented to find proper laser parameters that will result in minimal collateral damage for dermis ablation and separation. Finally, separation of dermis layers was demonstrated with minimum thermal damage and the layer uniformity was inspected.

2. METHODS & MATERIALS

2.1 Experimental Setup

For the USP laser experimental setup, four main parts - a USP laser system, a beam delivery system, a 3-axis motorized high speed high precision translation stage and a whole control system are included. The USP laser is a commercial Erbium doped fiber laser from Raydiance, Inc. The laser outputs pulses with repetition rate tunable between 1 Hz and 500 kHz. The output pulse energy is variable from 1 to 5 μJ. The laser central wavelength is 1552 nm and its pulse width is 900 fs. In the beam delivery system, the laser beam was focused to the target through an objective lens (Mitutoyo M Plan Apo NIR 20x, NA = 0.40, f_L =20 mm) as shown in Fig. 1. The laser beam before the lens is about 10 mm in diameter and the diffraction-limit focal spot diameter ($2.44\lambda f_L / D$) in free space is estimated as 8 μm. A digital power meter was used to measure the laser power loss in the beam delivery system. It is found that the total loss is about 50%, mainly due to reflection and absorption. Such a loss has been accounted for in the irradiation pulse energy values stated hereafter.

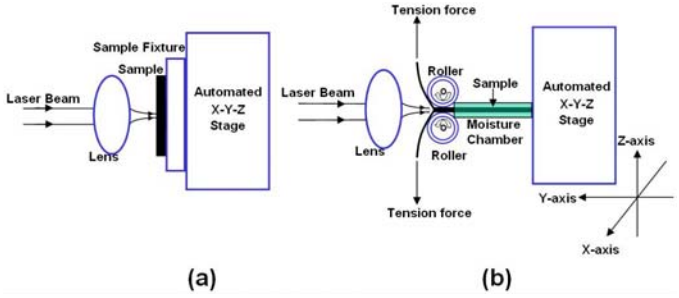

Figure 1. Experimental setups.

The whole control system is a RayOS^{TM} laptop interface which controls the laser output parameters (mainly pulse energy and repetition rate) as well as the motion of the 3-axis precision compact linear stage (VP-25XA, Newport). The work stage for mounting a tissue sample was fixed to the 3-D automated translation stage through which the alignment of optics and laser scanning were realized. There is a constant transition time for each axis of the stage when in motion. There are two designs for the work stage in this study. Figure 1(a)

shows the schematic diagram of experimental setup I with a plate fixture for sample mounting. This setup is simple and was used for characterizing the single line scanning ablation features.

To separate a piece of dermis into two layers, it requires tens of thousands of ablation lines and the process is very time consuming. A wet tissue mounting on the simple plate fixture was apt to dehydrate and deform because of the stage movement. In order to avoid the deformation, a moisture chamber that keeps the tissue wet during the laser processing was utilized as sketched in Fig. 1(b). A tissue feeding and pulling scheme was also designed in experimental setup II as shown in Fig. 1(b) such that the separation interface was always exposed to the laser focal spot through the pulling of two opposite tension forces. Therefore, one does not have to focus the beam into deep tissue and the strong attenuation of biological tissues against light is not a concern. With laser ablation at the exposed interface, the two opposite tension forces pull and split the dermis into two separate layers. An evacuator system (FX225, EDSYN) which is not shown in Fig. 1 was also employed to collect plasma plume residue and debris during the laser processing.

2.2 Tissue Samples

In this study, donor dermal tissues were used. The wet human dermis samples were prepared and provided by professionals from the project sponsor - MTF. The donor skin tissue was processed with a series of soak processing - sodium chloride, triton and finally disinfection soak to get epidermis removed and the processed wet tissue sample was whole dermis. The dermal tissue samples are about 2 mm thick and precut into about 10 mm long and 5 mm wide.

Like most natural objects the human skins have spectral variability which is in this case mainly due to amount, density, and distribution of melanin. The skin can be described as an optically inhomogeneous material because under the surface there are colourant particles which interact with light, producing scattering and colouration. It is well known that light scattering in biological tissues is very strong [21]. At wavelength 1552 nm, water absorption in wet dermis is also significant.

2.3 Microscopy & Measurements

Immediately following the ablation experiment, the micro topography and surface quality of the ablated tissue sample were examined immediately by an upright digital microscope (National Optical DC3-156-S). After that the treated tissue samples were fixed in 2% phosphate buffered glutaraldehyde for 2 hours, and rinsed twice in phosphate buffer and dehydrated in ethanol. After critical point drying, the tissue samples were checked by a scanning electron microscopy (SEM) (AMRAY 1830I). For the histological evaluation, the ablated samples were routinely dehydrated in a series of graded ethanol. Then the samples were fixed in paraffin wax and sectioned into 10μm-thick slices. After that, the slices were stained with Hemaoxylin and Eosin (H&E) for light microscopic evaluation. The analysis and photograph were performed by a Nikon ECLIPSE E600 microscope system. The thickness of the separated samples was measured by a vernier caliper.

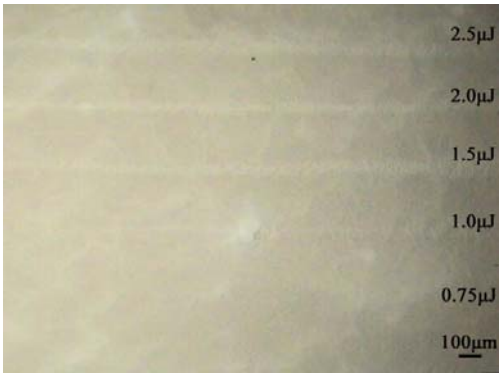

Figure 2. Microscopic view of wet tissue ablation lines with different irradiation pulse energies.

3. RESULTS AND DISCUSSION

3.1 Line Scanning and Ablation Threshold

To enable practical tissue separation, ablation features of surface line scanning and the ablation threshold of the wet human dermis must be understood first. The main parameters that affect the ablation include irradiation pulse energy, pulse repetition rate and speed of scanning. The irradiation pulse energy, E that is 50% of the laser output energy, determines whether the incident laser fluence is above the critical value that plasma-mediated ablation occurs. The pulse overlap rate is the ratio of the pulse repetition rate, f , over the moving speed of work stage, s (pulses per unit length) and it determines the pulse overlap intensity.

Before the ablation scanning, the focal plane was adjusted in the following steps. First the laser beam was focused to the sample surface until green light (i.e., third-harmonic generation) could be seen near the sample surface. Then the sample was slowly moved towards the beam; and one could see that the green light dimmed. When the green light was completely distinguished and a bright plasma spark could be seen, it indicated that plasma-mediated ablation generated. Finally an ablation line is formed when the sample was line scanned and continuous sparks could be observed during the processing period.

Figure 2 shows a picture (40X magnification) took by the digital microscopy for five laser scanned lines on a wet dermis surface with different irradiation pulse energies (0.75 μJ - 2.5 μJ). The pulse repetition rate was 500 kHz and the moving speed of the stage was 25 mm/s. Thus, the pulse overlap rate

was 20 pulses/μm. The imprints shown in Fig. 2 reflect the generated ablation lines. The width of the imprints increases as the pulse energy increases and is in the range from 30 to 50 μm. Under the microscopy, the width of the ablation lines is very uniform. However, the imprint should not be used as an accurate measurement of the ablation line width because the imprint may be inflated due to many factors such as bumps or water evaporation imprints.

Fine inspections of the ablation lines are conducted by the SEM measurement and four representative SEM images are shown in Fig. 3 for the four ablation lines generated with irradiation pulse energy 1.0 - 2.5 μJ, respectively. From the top view images in Figs. 3 (a) and (b), one can measure the average ablation line width as 18.5±1.3 μm and 15.6±0.7 μm for the cases of 2.5 and 2.0 μJ irradiation pulse energies, respectively. While the cut width using mechanical tools such as general surgical blade or scalpel is in the range from 100 μm to 1 mm [16]; so the USP laser ablation is more precise and results in less waste. Figures 3 (c) and (d) are views with a tilt angle for the ablation lines of 1.5 and 1.0 μJ irradiation pulse energies, respectively. Comparing Figs 2 and 3, obviously the SEM measurement is more accurate and the line widths in Fig. 2 are inflated and should not be adopted.

For laser pulses with a Gaussian spatial beam profile, the feature size obtained is related to the maximum laser fluence, F_0, on the samples surface. In laser ablation, the effective radius, r_{eff}, of the focal spot for experiment can be calculated directly from the following formula [22]:

$$D^2 = 2r_{\text{eff}}^2 \ln(\frac{F_0}{F_{\text{th}}}), \quad (1)$$

where D is the diameter of the ablation crater and F_{th} is the ablation threshold fluence. Thus, the effective radius of the laser focus spot needed for fluence calculations can be calculated from the slop of a plot of experimental datas. For laser pulses with a Gaussian spatial beam profile, the maximum irradiation fluence F_0 can be calculated from the irradiation pulse energy E as

$$F_0 = \frac{2E}{\pi r_{\text{eff}}^2}. \quad (2)$$

An ablation line consists of continuously ablated craters along the laser scanning direction. When the pulse overlap rate is so intense that no individual crater can be distinguished (such as displayed in Fig. 3), the ablation line width is then equivalent to the diameter of the ablated crater generated by N repeated pulses. The equivalent pulse number can be approximated by

$$N = 2r_{\text{eff}} f / s. \quad (3)$$

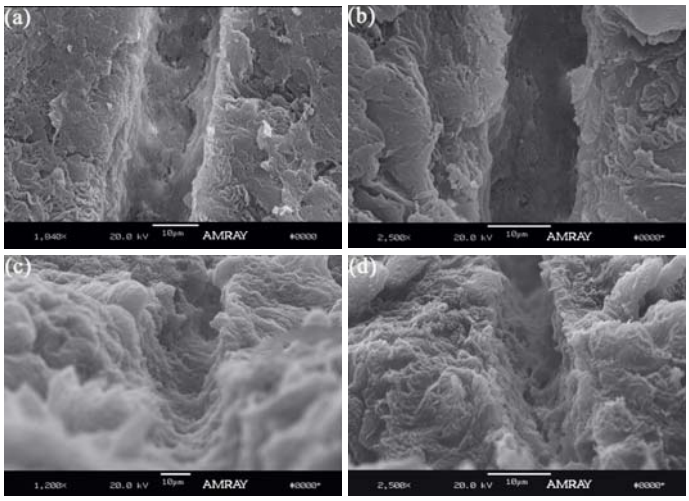

Figure 3. SEM images of surface single line ablation of wet dermis (20 pulses/μm) (a-b: top view for 2.5 μJ and 2.0 μJ, respectively; c-d: tilt view for 1.5 μJ and 1.0 μJ, respectively.)

Figure 4 plots the relationship - the square of the ablation line width versus the logarithm of irradiation pulse energy for three different pulse overlap rates. As pointed out by Bonse et al. [23], the data at high fluence points should be excluded from linear fitting because the deviation of the intensity from the Gaussian distribution at the "edge" of high fluence beam will lead to nonlinearity. It should be mentioned that the accumulated fluence for the present ablation lines is very high because the equivalent pulse number N is very large as calculated in Table 1. Thus, only low fluence points are adopted for the linear fitting to obtain the slopes of the three curves in Fig. 4, in particular for the curve with 20 pulses/μm pulse overlap rate. The calculated effective radii for the focal spots with different pulse overlap rates and the corresponding equivalent pulse number are listed in Table 1. It is seen that the effective spot size (9 - 17 μm) is bigger than the diffraction-limit spot size (8 μm) in free space. This is consistent with the result by Mullan et al. [24] and Choi et al. [25] for polymers and can be attributed to the strong scattering of light on the rough dermis surface. When the pulse overlap rate is just 5 pulses/μm, it is seen that the calculated effective radius is close to the diffraction-limit prediction. With increasing pulse overlap rate, the accumulated fluence increases and the deviation between the calculated effective radius and the diffraction-limit prediction widens.

The fluence can be calculated by equation (2) after obtaining the effective focal radius and the thresholds for different pulse overlap rates can be acquired by extending the fitted lines in Fig. 4 to intersect with the abscissa. Table 1 also lists the ablation thresholds for the three different pulse overlap rates. Clearly the ablation threshold decreases as the pulse overlap rate increases because of incubation effect [26]. The affect of incubation on ablation threshold can be quantified by

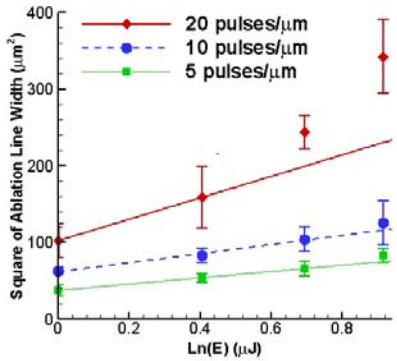

Figure 4. Effect of irradiance energy on ablation line width.

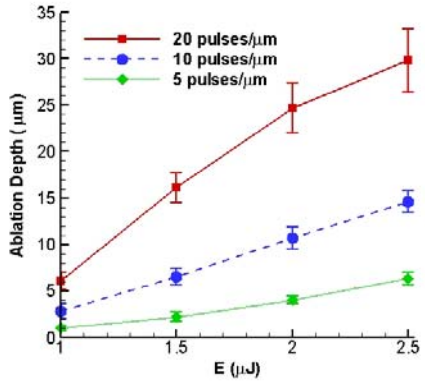

Figure 5. Single line ablation depth versus irradiance energy.

a relationship in the form as

$$F_{\text{th}}(N) = F_{\text{th}}(1)N^{\xi-1}, \quad (4)$$

where $F_{th}(1)$ and $F_{th}(N)$ refer to the ablation threshold due to a single pulse and N pulses, respectively. The exponent ξ is the so-called incubation factor. Using the data in Table 1, a least-squares fitting line of $\ln(NF_{th}(N))$ versus $\ln(N)$ can be drawn (not presented here) and the slope yields an incubation factor ξ = 0.46±0.03. Therefore, the ablation threshold for the wet human dermis is determined as $F_{th}(1)$ = 9.65±1.21 J/cm^2. The uncertainties are obtained using the methods described in refs [27, 28]. The plasma-mediated ablation threshold is slightly different with some other soft tissue, like brain tissue [3] and bovine neural tissue [8]. And this may owe to the difference of laser pulse duration, wavelength and the tissue properties. Although the fluence is not very high, the energy flux in the focal spot is above 10^{12} W/cm^2, which is hard to be achieved by CW or long pulsed lasers for thermal ablation.

Table 1. Effective focal spot radii and ablation thresholds

Pulse overlap rate (pulses/μm)	5	10	20
Equivalent pulse number	45	110	336
Effective focal spot radius (μm)	4.5	5.5	8.4
Ablation threshold F_{th} (J/cm^2)	1.27	0.75	0.43

Figure 5 shows the ablation depth change with the irradiation pulse energy for different pulse overlap rates in the situation of single line scanning ablation. For each ablation depth datum, three samples were measured to obtain the average value and the uncertainty. It should be noticed that in the preparation of fixing and drying for SEM examination, the samples may be somewhat distorted and the distortion affects the measurement accuracy as well. From Fig. 5 it is seen that the ablation depth increases with the irradiation pulse energy. Although different models relating the ablation mass to the energy delivered to the material have been proposed, none of them completely agrees with experimental results because the assumptions made are often satisfied for the entire range of radiant exposures over which the mass removal data are collected, such as shielding-effects [14, 15]. But our results show the same tendency with some previous studies by USP laser [8]. It is known that the pulse overlap rate increases with the pulse repetition rate but decreases with the scanning speed, and the ablation progress is linearly proportional to the scanning speed. For a fixed scanning speed, the ablation production efficiency increases with increasing pulse energy and repetition rate.

3.2 Histological Evaluations

In order to check the degree of thermal damage and find the proper laser parameters for tissue separation, the histology of the line scanning ablated samples was analyzed. Figure 6 shows the sectional view (200X magnification) of 12 H&E stained wet dermis samples ablated with single line surface ablation with different laser parameters. The selected pulse energies are 1.5, 2.0 and 2.5 μJ, respectively. The pulse overlap rates are 0.8, 5, 10 and 20 pulses/μm, respectively. The irradiation surface in the pictures faces down. Thermal damaged zone is visualized by the shadow area, because the elastic fibers in the damaged zone are no longer apparent, having been converted into an amorphous, coagulated mass. As observed from Fig. 6, no thermal damage or structure change occurs in the dermis when the pulse overlap rate is 5 pulses/μm and below, even in the case of high irradiation pulse energy (2.5 μJ). When the pulse overlap rate is 10 pulses/μm and above, however, a clear thermal damage zone is observable, in particular when the pulse energy is 2.0 μJ and above. The higher the pulse overlap rate or the higher the pulse energy, the larger and the severer (darker) is the thermal

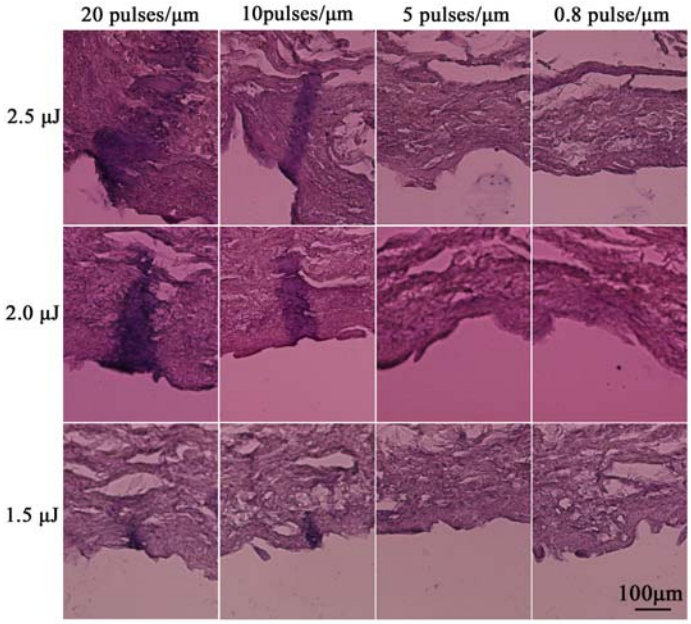

Figure 6. Histological analysis of single line surface ablation.

damaged zone. Hence, the accumulation of irradiation fluence is the key factor for causing thermal damage. In order to eliminate or minimize thermal damage, operation with a lower pulse overlap rate is essential. For the cases studied here, a pulse overlap rate up to 5 pulses/μm is safe for single line ablation.

The study by Suhm et al. [29] also showed no thermal damage signs in picosecond laser ablation of neural tissue. Kautek et al. [30] reported a damage zone less than 0.5 μm in the ablation of human corneas using a femtosecond pulsed laser. Girard et al. [31] claimed approximately 14 μm damage zone in the ablation of osseous tissues using a femtosecond Ti:Sapphire laser. When long pulsed lasers are utilized, thermal damage zone is more profound. For example, Walsh et al. [32] found that the damage zone jumped from 50 to 750 μm when the pulse duration increased from 2 μs to 50 ms using CO_2 lasers.

In order to achieve practical tissue separation or cutting, ablation scanning of multiple lines is required. As shown in Fig. 7, some representative histological results of multi-line ablation are compared and evaluated, where the sectional views (200X magnification) of 16 ablation processed tissue samples with different laser parameters are illuminated. Each tissue sample was repeatedly line scanned for 100 times with experimental setup II. During the processing, the ablation interface was always renewed via the tension through the two opposite tension forces. The selected pulse energies are 1.0, 1.5, 2.0 and 2.5 μJ, respectively. The pulse overlap rates are 0.8, 5, 10 and 20 pulses/μm, respectively. The irradiation surface in each picture faces up and arrows indicate the locations of the ablation cut in each picture. Now clear cuts to a

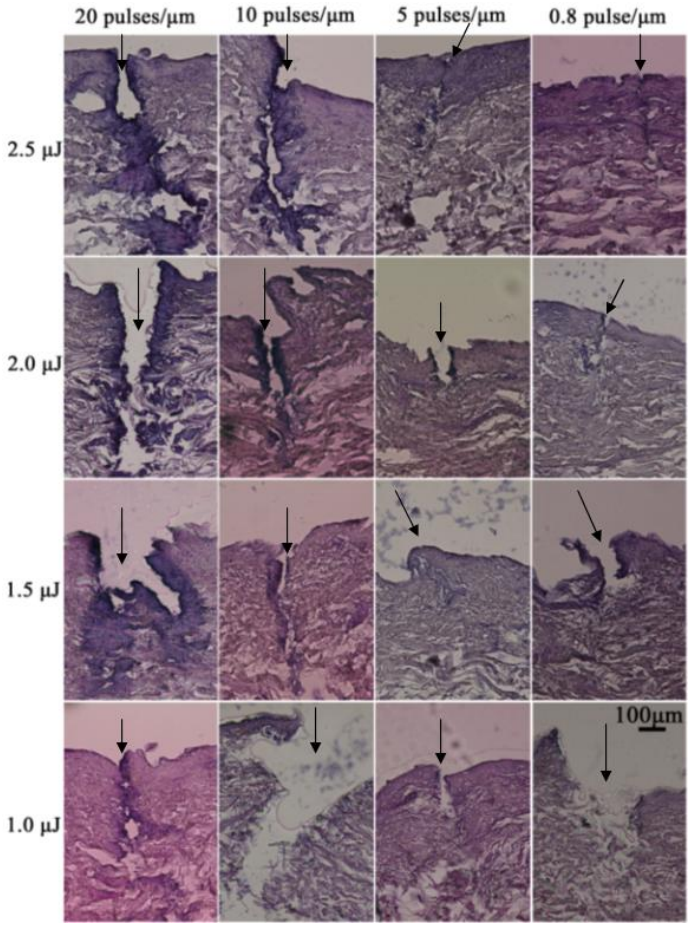

Figure 7. Histological analysis of multi-line ablation on wet tissue.

certain depth in all the samples are observed. Comparing Figs. 6 and 7, the underlying thermal damages in the cases of multi-line ablation are smaller than those in the cases of single line ablation, because the accumulation of the multi-line energy will take away the material in the underlining thermal damage zone. In practical tissue separation or cutting, the underlying damage is not a concern because the tissue has to be cut through.

The sizes of the lateral thermal damage zone around the cut edge for the laser parameter sets considered in Fig. 7 are listed in Table 2. The thermal damage behavior for the multi-line scanning cases is very similar to that observed in the single line scanning results, even though the accumulated fluence in multi-line scanning is many times stronger than the single line scanning. The reason is that between two successive scans, the lateral accumulation of thermal energy is trivial because the energy has been dissipated into the surroundings. It should be noticed that in the cases of multi-line ablation with pulse overlap rate 5 pulses/μm, however, lateral thermal damage is observed within a 10 μm zone when the irradiation pulse energy is 2.0 μJ or above, and the damage is reduced to 2-3 μm when the irradiation pulse energy is below 2.0 μJ. This is because the accumulated energy between two successive scans

Table 2. Lateral thermal damage zones resulted from 100 line ablation

Pulse overlap rate / Pulse energy	20 pulses/μm	10 pulses/μm	5 pulses/μm	0.8 pulse/μm
2.5 μJ	67±10 μm	40±8μm	8±3 μm	6±4 μm
2.0 μJ	54±10 μm	38±8 μm	6±4 μm	4±4 μm
1.5 μJ	52±8 μm	18±5 μm	3±2 μm	3±3 μm
1.0 μJ	26±6 μm	3±2 μm	2±2 μm	2±2 μm

has not been fully dissipated yet. This problem can be resolved by delaying the repeated scanning time.

Apart from the qualitative examination, Fig. 7 also shows the cut (ablation) depths for different pulse overlap rates and pulse energies. It is seen that the ablation depth generally increases as the pulse energy and/or overlap rate increase. In the current experiments, two clamps were used as the tension forces and the forces were not optimized in line with the single line ablation depth. Thus, the cutting depth due to multi-line ablation is not a simple multiplication of corresponding single line ablation depth. For example, the 100-line ablation depth for the picture in Fig. 7 with pulse overlap rate 5 pulses/μm and irradiation pulse energy 2.0 μJ is only 210 μm although its single line ablation depth from Fig. 5 reaches to 4.0 μm. Other reasons that could reduce the line ablation depth in the repeated line ablation include beam block by the edges of the prior ablation grooves or by the generated residues and debris. It should also be mentioned that in the preparation of samples for the histological view, the samples might be somewhat distorted and this may affect the measurement accuracy as well.

The cutting efficiency is defined as the amount of mass removed per unit energy delivered to the tissue. Since the sample widths to be scanned in the experiment are the same, the cutting efficiency can be defined by the cut depth per unit energy delivered to the tissue and it is directly proportional to the ablation depth and scanning speed. It is desirable to operate the laser tissue processing system at high irradiation pulse energy, high pulse repetition rate and high speed of scanning, because high pulse energy can enlarge the ablation depth and high repetition rate and high speed of scanning can shorten the processing time for each line scanning. In the same time, the pulse overlap rate must be controlled to avoid thermal damage. In summary, an optimal set of operation parameters for wet dermis cutting and separation is recommended as follows: irradiation pulse energy = 1.5 μJ, stage moving speed = 25 mm/s (the maximum of the current instrument), pulse repetition rate = 125 kHz, and pulse overlap rate = 5 pulses/μm.

3.3 Tissue Separation

After obtaining the proper laser parameters for tissue separation, thin layer separation of wet dermis is demonstrated in Fig. 8. The tissue sample was processed with experimental

(a) Separated tissue layers (b) Thinner layer separation

Figure 8. Wet tissue separations by USP laser ablation.

setup II (see Fig. 1(b)) with 5 pulses/μm pulse overlap rate and 1.5 μJ pulse energy. Figure 8(a) shows the two separated layers that are about 500 μm and 800 μm thick with about 10% unevenness, respectively for the upper and lower pieces. The original wet dermis sample before laser ablation was 30 mm long, 8 mm wide and 2 mm thick. Both layers are slightly deformed because of tension forces applied during the feeding and pulling process.

Furthermore, the separated dermis layers can be further split for multiple usages. Figure 8(b) shows the partially separated result of another dermis layer of 20 mm long, 6 mm wide and 560 μm thick with the same laser parameters. The thickness of the further separated dermis thin layer is about 220 μm with about 20 μm unevenness. Inspection of the separated layers in Figs. 8, no obvious thermal charring or melting was found. However, some parts of the surfaces turned into yellow; minor thermal damage to the level of about 0.01 mm might have happened. The main reasons include that the current tissue feeding and pulling scheme design is not very precise and optimal; and adjustments during the processing were needed to keep the joined tissue in ablation area, which may cause unexpected irradiation of separated edge area and prolongs the time of processing. Further improvement of the experimental set up to minimize the thermal damage and distortion to the separated dermis layer is the future direction.

4. CONCLUSION

In vitro human dermis separation via USP laser plasma-mediated ablation has successfully completed. Firstly, parametric study of surface line scanning of wet dermis tissue was investigated and the obtained ablation threshold was 9.65±1.21 J/cm^2 for equivalently single pulse ablation. And the incubation factor was found as 0.46. Then histological evaluations were performed to find proper laser parameters for dermis separation with minimal thermal damage. No thermal damage was found in the single line ablation results when the pulse overlap rate was not over 5 pulses/μm. Even in multi-line ablation, the lateral thermal damage zone was generally within 5 μm in the results with 100 continuously repeated line scans for pulse overlap rate within the range of 0.8 - 5 pulses/μm and 1.0 - 1.5 μJ pulse energy. After that, the effects of laser pulse energy and pulse overlap rate on ablation efficiency were studied. Finally real human dermis samples were separated

with USP laser ablation and a thin layer 220 μm thick was obtained without obvious thermal charring or melting.

ACKNOWLEDGMENTS

This work was supported by the Musculoskeletal Transplant Foundation. The authors are grateful to Michael Schuler, Arthur Gertzman, Alex Scozzarro at MTF; to Greg Spooner at Raydiance, Inc.; and to Tin O. Khor and Siwang Yu at Rutgers University, for assisting with the experiments and examinations.

REFERENCES

[1] Niemz, M.H., 2003, Laser-tissue interactions: fundamentals and applications, 3rd ed., Springer, Heidelberg.

[2] Niemz, M.H., Klancnik, E.G., Bille, J.F., 1991, "Plasma-mediated ablation of corneal tissue at 1053 nm using a Nd:YLF oscillator/regenerative amplifier laser", Lasers in Surgery and Medicine, **11**(5), pp. 426-431.

[3] Fischer, J.P., Dams, J., Götz, M.H., Kerker, E., Loesel, F.H., Messer, C.J., Niemz, M.H., Suhm, N., Bille, J.F., 1994, "Plasma-mediated ablation of brain tissue with picosecond laser pulses", Applied Physics B, **58**, pp. 493-499.

[4] Kim, K.H. and Guo, Z., 2004, "Ultrafast radiation heat transfer in laser tissue welding and soldering", Numerical Heat Transfer, Part A: Applications, **46**(1), pp. 23-46.

[5] Guo, Z., Wan, S.K., August, D.A., Ying, J., Dunn, S.M., Semmlow, J.L., 2006, "Optical imaging of breast tumor through temporal log-slope difference mappings", Computers in Biology and Medicine, **36**(2), pp. 209-223.

[6] Quan, H. and Guo, Z., 2004, "Fast 3-D optical imaging with transient fluorescence signals," Optics Express, **12**(3), pp. 449-457.

[7] Moss, J.P., Patel, B.C., Pearson, G.J., Arthur, G., Lawes, R.A., 1994, "Krypton fluoride excimer-laser ablation of tooth tissues: precision tissue machining", Biomaterials, **15**(12), pp. 1013-1018.

[8] Loesel, F.H., Fischer, J.P., Götz, M.H., Horvath, C., Juhasz, T., Noack, F., Suhm, N., Bille, J.F., 1998, "Non-thermal ablation of neural tissue with femtosecond laser pulses", Applied Physics B, **66**, pp.121-128.

[9] Chen, S.C., Kancharla, V., Lu, Y., 2003, "Laser-based microscale patterning of biodegradable polymers for biomedical applications", International Journal of Materials & Product Technology, **18**(4-6), pp. 457-468.

[10] Aguilar, C.A., Lu, Y., Mao, S., Chen, S., 2005, "Direct micro-patterning of biodegradable polymers using ultraviolet and femtosecond lasers", Biomaterials, **26**(36), pp. 7642-7649.

[11] Huang, H., Guo, Z., 2009, "USP laser PDMS thin-layer separation and micro-fabrication", J. Micromech. Microeng., **19,** 055007 (9pp).

[12] Liu, Y.M., Sun, S., Singha, S., Cho, M.R., Gordon, R.J., 2005, "3D femtosecond laser patterning of collagen for directed cell attachment", Biomaterials, **26**(22), pp. 4597-4605.

[13] Hallgren, C., Reimers, H., Chakarov, D., Gold, J., Wennerberg, A., 2003, "An in vivo study of bone response to implants topographically modified by laser micromachining", Biomaterials, **24**(5), pp. 701-710.

[14] Welch, A.J., and van Gemert, M. J.C., 1995, Optical-thermal response of laser-irradiated tissue, Plenum Press, New York.

[15] Vogel, A. and Venugopalan, V., 2003, "Mechanisms of pulsed laser ablation of biology tissues", Chemical Review, **103**, pp. 577-644.

[16] Schuler, M., Gertzman, A.A., 2007, Private communications, The Musculoskeletal Transplant Foundation.

[17] Kearney, J.N., 2005, "Guidelines on processing and clinical use of skin allografts", Clinical Dermatology, **23**, pp. 357-464.

[18] Costantino, P.D., Govindaraj, S., Hiltzik, D.H., Buchbinder, D., Urken, M.L., 2001, "Acellular dermis for facial soft tissue augmentation preliminary report", Archives of Facial Plastic Surgery, **3**(1), pp. 38-43.

[19] Spear, S.L., Parikh, P.M., Reisin, E., Menon, N.G., 2008, "Acellular dermis-assisted breast reconstruction", Aesthetic Plastic Surgery, **32**(3), pp. 418-425.

[20] Buck, B.E., Malinin, T.I., 1994, "Human bone and tissue allografts preparation and safety", Clinical Orthopaedics and Related Research, **303**, pp. 8-17.

[21] Troy, T.L., Thennadil, S.N., 2001, "Optical properties of human skin in the near infrared wavelength range of 1000 to 2200 nm", Journal of Biomedical Optics, **6**(2), pp. 167-176.

[22] Baudach, S., Bonse, J., Kautek, W., 1999, "Ablation experiments on polyimide with femtosecond laser pulses", Applied Physics A, **69**, pp. S395-S398.

[23] Bonse, J., Wrobel, J.M., Krüger, J., Kautek, W., 2001, "Ultrashort-pulse laser ablation of indium phosphide in air", Applied Physics A, **72**, pp. 89-94.

[24] Mullan, C., O'Connor, G.M., Favre, S., Ilie, D., Glynn, T.J., 2007, "Estimating spot size and relating hole diameters with fluence and number of shots for nanosecond and femtosecond laser ablation of polyethylene terephthalate", Journal of Laser Applications, **19**(3), pp. 158-164.

[25] Choi, H.W., Johnson, J.K., Nam, J., Farson, D.F., Lannutti, J., "Structuring electrospun polycaprolactone nanofiber tissue scaffolds by femtosecond laser ablation", Journal of Laser Applications, **19**(4), pp. 225-231.

[26] Rosenfeld, A., Lorenz, M., Stoian, R., Ashkenasi, D., 1999, "Ultrashort laser pulse damage threshold of transparent materials and the role of incubation", Applied Physics A, **69**, pp. S373-S376.

[27] Higbie, J., 1991, "Uncertainty in the linear regression slope", American Journal of Physics, **59(2)**, pp. 184-185.

[28] Holman, J.P., 2001, Experimental methods for engineers, 7th ed., McGraw Hill, Boston.

[29] Suhm, N., Götz, M.H., Fischer, J.P., Loesel, F., Schelgel, W., Sturm, V., Bille, J., Schröder, R., 1996, "Ablation of neural tissue by short pulsed laser: A technical report", Acta Neurochirurgica **138**(3), pp. 346-349.

[30] Kautek, W., Mitterer, S., Krüger, J., Husinsky, W., Grabner, G., 1994, "Femtosecond-pulse laser ablation of human corneas", Applied Physics A, **58**, pp. 513-518.

[31] Girard, B., Yu, D., Armstrong, M.R., Wilson, B.C., Clokie, C.M.L., Miller, R.J.D., 2007, "Effects of femtosecond laser irradiation on osseous tissues", Lasers in Surgery and Medicine, **39(3)**, pp. 273-285.

[32] Walsh, J.T. Jr., Flotte, T.J., Anderson, R.R., Deutsch, T.F., 1988, "Pulsed CO2 laser tissue ablation: effect of tissue type and pulse duration on thermal damage", Lasers in Surgery and Medicine, **8**(2), pp. 108-118.